

ISSN 0280-5316  
ISRN LUTFD2/TFRT-5509--SE

# Active Damping of Subsynchronous Resonance

Erik Gustafson

Department of Automatic Control  
Lund Institute of Technology  
July 1994

<b>Department of Automatic Control</b> <b>Lund Institute of Technology</b> P.O. Box 118 S-221 00 Lund Sweden	<i>Document name</i> MASTER THESIS	
	<i>Date of issue</i> July 1994	
	<i>Document Number</i> ISRN LUTFD2/TFRT--5509--SE	
<i>Author(s)</i> Erik Gustafson	<i>Supervisor</i> Karl Johan Åström, Anders Åberg ABB	
	<i>Sponsoring organisation</i>	
<i>Title and subtitle</i> Active Damping of Subsynchronous Resonance		
<i>Abstract</i> <p>This report deals with the damping of subsynchronous oscillations in power systems. The method is based on estimation of the generator rotor angle and shaft speed, by measuring the line current and the voltage across a phase-compensating series capacitor. These two signals are probably not sufficient, so a line-to-ground voltage measurement is added. However, this means increased costs. A thyristor-controlled series capacitor, TCSC, is used as a voltage source in serial with the line. A control law that uses the estimated angle and shaft speed determines the TCSC voltage, in order to create an actively damping torque.</p> <p>The model is described in Chapter 2, This model holds only one oscillative mode. Simulations of a more sophisticated model, which has several oscillative modes, will thus be necessary. A stability analysis of the linearized model is carried out in Chapter 4. In Chapter 5, control strategies are derived, of which the first one is used in the rest of the report. The estimation problem seems to be the most crucial one. Different methods are discussed in Chapter 7. The linear Kalman estimator is chosen for the suggested controller structure in Chapter 8.</p> <p>The problems of stability and parameter robustness are not completely analysed. More work needs to be done in this field.</p>		
<i>Key words</i>		
<i>Classification system and/or index terms (if any)</i>		
<i>Supplementary bibliographical information</i>		
<i>ISSN and key title</i> 0280-5316		<i>ISBN</i>
<i>Language</i> English	<i>Number of pages</i> 36	<i>Recipient's notes</i>
<i>Security classification</i>		



# Contents

<b>1</b>	<b>Introduction</b>	<b>2</b>
1.1	Three Phenomena . . . . .	2
1.2	The Problem . . . . .	3
<b>2</b>	<b>The model</b>	<b>4</b>
2.1	The Electrical System . . . . .	4
2.2	The Mechanical System . . . . .	5
2.3	The Complete Model . . . . .	5
<b>3</b>	<b>Torsional Interaction Simulations</b>	<b>7</b>
<b>4</b>	<b>The Linearized Model</b>	<b>9</b>
4.1	Eigenvalue Analysis . . . . .	9
<b>5</b>	<b>Control Strategies</b>	<b>12</b>
5.1	Increased Damping . . . . .	12
5.2	Controlling the Stored Energy . . . . .	13
<b>6</b>	<b>Some Key Questions</b>	<b>15</b>
6.1	Question 1 . . . . .	15
6.2	Question 2 . . . . .	16
6.3	Question 3 . . . . .	16
6.4	Conclusions . . . . .	16
<b>7</b>	<b>Estimation Strategies</b>	<b>17</b>
7.1	Stator Frame Estimation . . . . .	17
7.1.1	Rotor Angle Differentiation . . . . .	17
7.1.2	Stator Voltage Integration . . . . .	17
7.1.3	Stator Voltage Differentiation . . . . .	18
7.2	Rotor Frame Estimation . . . . .	18
7.2.1	Stator Voltage Differentiation . . . . .	18
7.2.2	Linear Estimation . . . . .	19
<b>8</b>	<b>Final Solution</b>	<b>21</b>
<b>A</b>	<b>Analytical Tools</b>	<b>22</b>
<b>B</b>	<b>Linearization Using MAPLE</b>	<b>23</b>
<b>C</b>	<b>Program Code</b>	<b>28</b>

# Chapter 1

## Introduction

The transmission capability of long transmission lines is limited by the reactive power consumption of the line. One way to get to grips with this problem is to compensate the inductive reactance of the line by inserting series capacitors. However, this gives rise to additional problems. The presence of a capacitor turns the line into a resonance circuit.

If a mechanical turbine-generator system has a torsional oscillatory mode of frequency  $\omega$  below the synchronous frequency  $\omega_N$ , the rotational motion may be slightly modified due to vibrations of frequency  $\omega$ . These vibrations will be transferred to the electrical system consisting of the generator and the transmission line. So, in addition to the  $\omega_N$  frequency component of the current, there will be components of the current of the two frequencies  $\omega_N + \omega$  and  $\omega_N - \omega$  as well. These frequencies are referred to as the supersynchronous and the subsynchronous frequency, respectively.

If the subsynchronous frequency is close to the resonance frequency of the electrical system then substantial stator current may occur. This causes an electrical torque that is transferred back into the mechanical system. The vibrations may be amplified, leading to shaft fatigue and fracture. In 1970 a turbine-generator unit in southern Nevada started to oscillate heavily when connected to a series capacitor compensated transmission line. The same thing occurred in 1971. In both cases the unit was shut down manually before an actual shaft fracture but the shaft material had experienced high cycle fatigue leading to plasticity.

### 1.1 Three Phenomena

A lot of time was spent trying to understand what had happened. The phenomenon was called subsynchronous resonance, SSR. There are basically three

forms of subsynchronous resonance, namely *Torsional Interaction*, *Induction Generator Effect* and *Torque Amplification*.

**Torsional Interaction** occurs when the synchronous frequency complement of a natural frequency of the mechanical turbine-generator system is close to the resonance frequency of the network. *Electrical oscillations are then transmitted to the mechanical system.* The synchronous frequency complement is the synchronous frequency  $\omega_N$  minus the natural mechanical frequency  $\omega$ .

**Induction Generator Effect** is said to occur if the virtual resistance for the total equivalent stator circuit becomes negative at some frequency in the subsynchronous range. The *negative resistance* is caused by the negative slip in the rotor circuit for subsynchronous frequencies. Induction Generator Effect is an electrical phenomenon, which can occur even if the rotational speed is constant.

**Torque Amplification** is a *transient phenomenon* where subsynchronous oscillations are excited by electrical or mechanical transients, for instance line short-circuits in the transmission system. If the conditions are close to subsynchronous resonance, very high torques may occur.

Oscillations caused by Torque Amplification grow very fast. For the Induction Generator Effect and the Torsional Interaction on the other hand, it takes several seconds for the oscillations to grow to a damaging level. This makes the oscillations easier to control.

The incidents in 1970 and 1971 lead to a lot of precautions to avoid accidents in the future. Thanks to that there have been no further severe incidents.

## 1.2 The Problem

This thesis deals with the problem of torsional interaction. What is sought is a way to create an active damping that eliminates heavy oscillations.

The villain concerning all kinds of subsynchronous resonance is that introduction of a series capacitor causes an electrical series resonance to occur in the transmission line. Without any special means, compensation is possible up to a certain maximum degree. If it is possible to have different compensation degrees for different frequencies, the compensation degree for the fundamental frequency (50 or 60 Hz) can be raised, whereas it is kept unchanged for subsynchronous frequencies. The system will still be stable. This can be achieved by introducing a virtual impedance by a feedback loop, which affects only subsynchronous frequencies.

Modification of the impedance is primarily used to prevent build-up of SSR oscillations from a steady-state condition. However, transients in the system may give rise to oscillations in the turbine-generator system. It is desirable that these are dampened more actively, because of the poor damping of the mechanical part of the system. Merely affecting the electrical part by means of a virtual impedance will not be sufficient.

Sophisticated methods to control the power transmission, including avoiding SSR incidents, are made possible by the introduction of the Thyristor Controlled Series Capacitor (TCSC). The TCSC introduces a thyristor controlled inductive path connected in parallel with the series capacitor. It becomes possible to control an additional charge beside the charge from the line current in the series capacitor. Thereby the capacitor voltage can be controlled from half-cycle to half-cycle of the main frequency. The fast control of the inserted voltage makes the TCSC suitable for an active control of the SSR phenomenon.

An equivalent way to describe the TCSC is as a voltage source in series with the line. This thesis discusses the problem of formulating a control strategy for the voltage source with the purpose to create damping torques in the generators.

Some constraints complicates the problem:

- The only signals measurable without additional investments are the line current and the capacitor voltage.
- The system can include many generators with different resonance frequencies.
- The configuration of the network changes all the time. Parallel lines are being switched in and out and the load varies.

The distance problem is probably not so severe, as the wavelength of line current and voltage is over 5,000 km (the waves travel almost at the speed of light). Difficulties with more than one generator and parallel lines are neglected in this thesis. If it is possible to find a control strategy for a system with only one generator and one transmission line, it might be tempting to try to handle the additional problems with a more complex system. The model used is thus the simplest possible where the problems with SSR may still occur.

- The system should be controlled at the capacitor, which may be located far away from the generator.

## Chapter 2

# The model

Extensive studies have been made of the SSR phenomena and it is important to be able to compare the results of these different studies. For this reason, the IEEE Subsynchronous Resonance Task Force has presented two benchmark models. These models should be as simple as possible but still be able to explain the problems with SSR. Experiment in this report is based on the first benchmark model for self-excitation studies. The model consists of two major part, a mechanical system and an electrical network, connected by a generator.

The generator design motivates that, as a first approximation, the three-phase system is assumed symmetric and the voltages and the currents can thus be totally determined by one complex voltage or current vector. This is described in [Elgerd] and [Ångquist1]. It is important to differ the rotor coordinate system from the stator coordinate system, whence the stator frame quantities are written with an upper index  $s$  and the rotor frame quantities with an  $r$

$$A^s = A^r e^{j\theta_s}$$

where  $\theta_s$  is the steady-state rotor angle in the stator frame, that is, the rotor angle in case of no torsional oscillations. Torsional oscillations can be described as oscillative disturbances from the steady-state position. The rotor angle is thus a relatively small oscillation  $\Delta\theta$  superposed on the steady-state angle  $\theta_s$ :

$$\theta = \theta_s + \Delta\theta$$

In the report all quantities are given in per unit (p.u.) [Elgerd, Ångquist1].

### 2.1 The Electrical System

The dynamical behaviour of the system with the stator and the transmission line can be represented by

a model with only one inductive component, one resistance and one capacitor connected in one end to a generator and in the other end to a stiff net. The stiff net is not affected by what happens in the network under consideration. See Figure 2.1, where

$x_L$	is the total inductive reactance,
$r_L$	is the total resistance,
$x_C$	is the capacitive reactance in the capacitor,
$i_L$	is the complex line current vector,
$u_C^s$	is the complex capacitor voltage vector,
$u_S^s$	is a controllable voltage source,
$\Psi_S^s$	is the rotor flux vector, and
$\Psi_B^s$	is the bus flux from the stiff net.

Kirchhoff's Voltage Law leads to the following equations:

$$\frac{1}{\omega_N} \frac{d\Psi_S^s}{dt} = \frac{x_L}{\omega_N} \frac{di_L^s}{dt} + r_L i_L^s + u_C^s - u_S^s + \frac{1}{\omega_N} \frac{d\Psi_B^s}{dt} \quad (2.1)$$

$$\frac{1}{\omega_N} \frac{du_C^s}{dt} = x_C i_L^s \quad (2.2)$$

The copper windings of the rotor makes it difficult to change the magnetic flux through it. The frequencies under consideration deviate at least 10 Hz from the synchronous frequency, and so they do not penetrate the rotor cage. The flux can therefore be regarded as fix in the rotor frame. This gives the flux in the stator frame:

$$\Psi_S^s = \hat{\Psi} e^{j\theta(t)} \quad (2.3)$$

$$\dot{\Psi}_S^s = j\dot{\theta} \hat{\Psi} e^{j\theta(t)} \quad (2.4)$$

The bus flux  $\Psi_B^s$  is assumed to be strictly synchronous and independent of the system:

$$\Psi_B^s = \hat{\Psi}_B e^{j(\theta_s(t) - \alpha)} \quad (2.5)$$

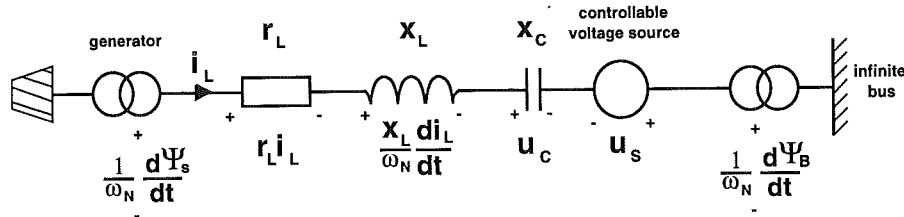


Figure 2.1: A schematic diagram of the electrical system.

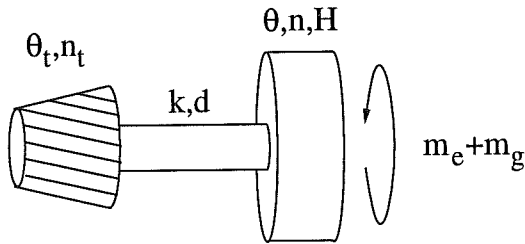


Figure 2.2: The mechanical turbine-rotor system.

If  $\hat{\Psi} = \hat{\Psi}_B$ , the load of the system depends on how much the bus voltage vector  $\frac{1}{\omega_N} \frac{d\hat{\Psi}_B}{dt}$  lags the generator voltage vector  $\frac{1}{\omega_N} \frac{d\hat{\Psi}_S}{dt}$ . A positive  $\alpha$  gives a power flow from the generator to the outer net, whereas a negative  $\alpha$  results in a power flow in the opposite direction. The generator works as a motor, that forces the turbine to rotate.

## 2.2 The Mechanical System

The mechanical system consists of a number of different turbines and a generator rotor, placed after each other and connected by different kinds of shafts. The system has many different oscillation modes. A model which has the same dynamical behaviour would be very sophisticated. A simplified model consists of only one turbine, a rotor, and a shaft. This gives only one oscillation mode. The rotation of the turbine affects the rotor as a mechanical torque. Further, there is an electrical torque from the network  $m_e$ , and possibly an additional torque  $m_g$ ; see Figure 2.2. This gives the second order torque equation for the rotor:

$$\frac{2H}{\omega_N} \frac{d^2\theta}{dt^2} = -d \left( \frac{d\theta}{dt} - \frac{d\theta_t}{dt} \right) - k(\theta - \theta_t) + m_e + m_g \quad (2.6)$$

Here,

- $\theta$  is the rotor angle,
- $\theta_t$  is the turbine angle,
- $H$  is the inertia constant of the rotor,
- $d$  is the damping coefficient of the shaft, and
- $k$  is the spring constant of the shaft.

The inertia constant of the turbine is said to be very large; this makes the turbine rotate at constant angular speed. Accordingly, the system has only one degree of freedom corresponding to torsional oscillations.

The coupling between the electrical and the mechanical system is given by the electrical torque:

$$m_e = Im(-i_L \hat{\Psi}_S^*) \quad (2.7)$$

The additional torque,  $m_g$ , is set to zero.

## 2.3 The Complete Model

The model is described by four differential equations.

$$\frac{di_L^s}{dt} = -\frac{\omega_N r_L}{x_L} i_L^s - \frac{\omega_N}{x_L} u_C^s + \frac{\omega_N \hat{\Psi}}{x_L} j e^{j\theta} \quad (2.8)$$

$$-\frac{\omega_N \hat{\Psi}_B}{x_L} j e^{j(\theta_s - \alpha)} n_t + \frac{\omega_N}{x_L} u_S^s$$

$$\frac{du_C^s}{dt} = \omega_N x_C i_L^s \quad (2.9)$$

$$\frac{d\theta}{dt} = \omega_N n \quad (2.10)$$

$$\frac{dn}{dt} = -\frac{k}{2H} (\theta - \theta_t) - \frac{\omega_N d}{2H} (n - n_t) - \frac{1}{2H} Im(i_L^s \hat{\Psi} e^{-j\theta}) \quad (2.11)$$

This is essentially two oscillators connected by some non-linear function. The coupling is, however, not



very tight. The eigenvalues of the linearized system are close to what they would be if the oscillators were totally separated.

The electrical oscillator is described by Equations 2.9 and 2.10:

$$\frac{d}{dt} \begin{bmatrix} i_L^s \\ u_C^s \end{bmatrix} = \begin{bmatrix} -\frac{\omega_N r_L}{x_L} & -\frac{\omega_N}{x_L} \\ \omega_N x_C & 0 \end{bmatrix} \begin{bmatrix} i_L^s \\ u_C^s \end{bmatrix} + \begin{bmatrix} f(\theta, n) \\ 0 \end{bmatrix} + \begin{bmatrix} \frac{\omega_N}{x_L} \\ 0 \end{bmatrix} u_S^s$$

The mechanical oscillator is described by Equations 2.11 and 2.12:

$$\frac{d}{dt} \begin{bmatrix} \theta \\ n \end{bmatrix} = \begin{bmatrix} 0 & \omega_N \\ -\frac{k}{2H} & -\frac{\omega_N d}{2H} \end{bmatrix} \begin{bmatrix} \theta \\ n \end{bmatrix} + \begin{bmatrix} 0 \\ g(\theta, i_L^s) \end{bmatrix}$$

The non-linear functions,  $f$  and  $g$ , describe the coupling between the two oscillators. The influence on the line current by the generator voltage and the stiff net is given by the function  $f$ , whereas the function  $g$  describes the electrical torque due to the line current and rotor flux. As mentioned before, currents and voltages are complex vectors. This actually gives six differential equations and, consequently, six states.

The following parameter values from the first benchmark model will cause resonance at the torsional oscillation frequency 25.55 Hz:

$$\begin{aligned} H &= 6.92s \\ k &= 946.12pu/rad \\ d &= 0.002056pu/(rad/s) \\ x_L &= 0.83pu \\ r_L &= 0.02pu \\ x_C &= 0.287pu \\ \hat{\Psi} &= 1pu \\ \omega_N &= 2 * \pi * 60rad/s \end{aligned}$$

## Chapter 3

# Torsional Interaction Simulations

The torsional interaction phenomenon can be visualized by simulating the model from Section 2.3. The simulation program Simnon is used for the simulations. The Simnon code is found in Appendix C.

All voltages and currents are complex, representing the symmetric three-phase system. The infinite bus is in the simulations represented by a 60 Hz synchronous rotating voltage source. The system works under no-load conditions but the simulations look almost the same when a power flow is introduced. This means that power is drawn out from the system by the outer net and it results in a synchronous current in the net.

The model was first simulated for two seconds, starting with the rotor angle a little disturbed. This was done in order to let the transient behaviour of the system stabilize a little. The state values after two seconds were used as initial values for all three simulations shown in this chapter. Figure 3.1 shows the

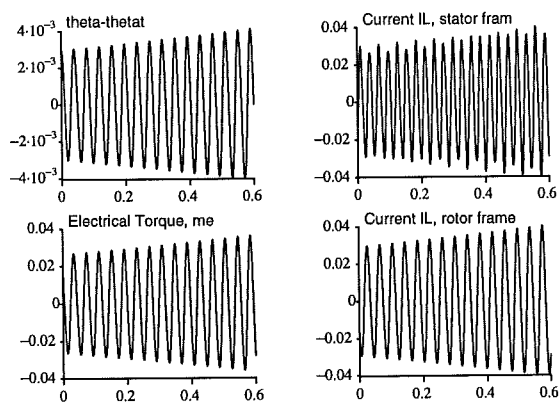


Figure 3.1: *The uncontrolled system at resonance. The mechanical resonance frequency 25.55 Hz is shown in three of the pictures, whereas the stator frame current, in the upper right picture, shows the synchronous frequency complements  $60 \pm 25.55$  Hz.*

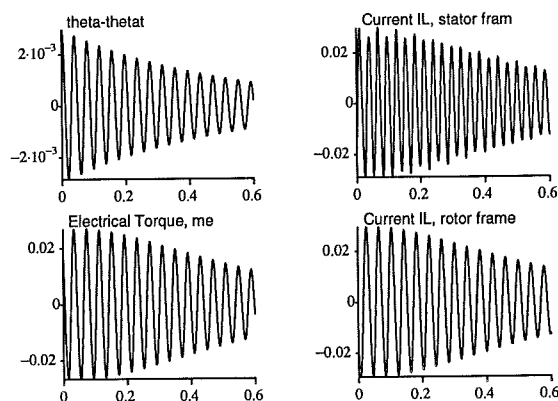


Figure 3.2:  *$d = 0.2$ . An increased damping makes the system stable.*

increasing oscillations of the system at resonance. The upper left picture, which shows the torsional oscillation  $\Delta\theta$ , and the two lower pictures, showing the electrical torque  $m_e$  and the line current in rotor coordinates  $i_L^r$ , all show oscillations of the resonance frequency of the mechanical system, 25.55 Hz. The upper right picture, the line current in stator coordinates, shows oscillations of two superposed frequencies 34 Hz and 86 Hz. These are the subsynchronous and the supersynchronous complementary frequency components  $60 \pm 25.55$  Hz.

In the simulation in Figure 3.1, the damping parameter was  $d = 0.002$ . The system can be stabilized by increasing the damping. In Figure 3.2,  $d = 0.2$ . The oscillations are damped nicely, and so are the complementary frequency components of the current, as can be seen in the rotor frame current diagram.

Another way to prevent the oscillations from increasing is to change the resonance frequency of the network by altering the capacitance. However, this affects the phase compensation level, and a very big change is necessary to make the system stable. Fur-

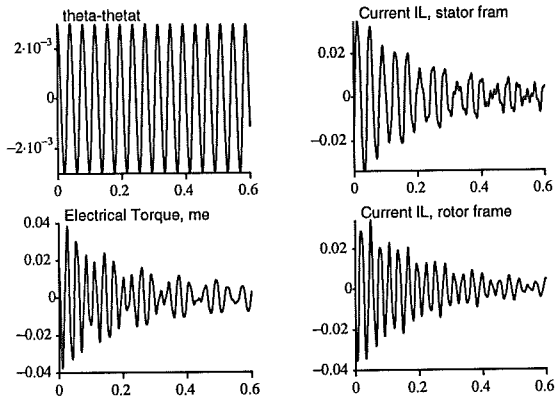


Figure 3.3: *A change in capacitance keeps the oscillations small, but they are not damped out efficiently.*

thermore, the poor damping of the mechanical system is not affected at all. If, for example due to a line failure, the system is already oscillating, the oscillations will last for a long time. In Figure 3.3 the capacitive reactance is changed from  $x_c = 0.287$  to  $x_c = 0.15$ .

A change in resistance will damp the current but will affect the mechanical oscillations only marginally more compared to a changed capacitance. Nevertheless, to introduce a virtual resistance for the sub-synchronous current, in combination with a virtual damping of the mechanical oscillations is probably the best solution. This is further motivated in Chapter 4.

## Chapter 4

# The Linearized Model

As long as the torsional oscillations are kept small, a linearized model tells a great deal about the stability of the system. This is one reason to look at the linearization of the model in Chapter 2. Furthermore, it is likely that a common linear feedback will be sufficient to make the non-linear system stable.

One problem with the linearization is the synchronous rotation of the rotor. In stator coordinates there is no steady state. However, if all states and signals are expressed in synchronously rotating coordinates, the synchronous signals will become constant. Now a new problem is introduced: -how are the measurement signals,  $u_C$  and  $i_L$ , transformed into these synchronous coordinates?

With  $\theta$  as the rotor angle in the rotating coordinate system, the linearized system reads

$$\begin{aligned} \dot{X} &= AX + BU \\ Y &= CX \end{aligned}$$

where

$$\begin{aligned} X &= (\Delta i_{lr} \Delta i_{lim} \Delta u_{cre} \Delta u_{cim} \Delta \theta \Delta n)^T \\ U &= (\Delta u_{sre} \Delta u_{sim})^T \\ Y &= (\Delta i_{lr} \Delta i_{lim} \Delta u_{cre} \Delta u_{cim})^T \end{aligned}$$

The matrices A, B, and C are shown in Appendix B.

### 4.1 Eigenvalue Analysis

The eigenvalues of the linearized system tells a great deal about the stability. The analysis is performed under no load conditions, which means that there is no power transmission. In this case  $i_{L0} = 0$  and  $u_{C0} = 0$ .

For the uncompensated case, that is, with no series capacitor, there are four eigenvalues or poles.

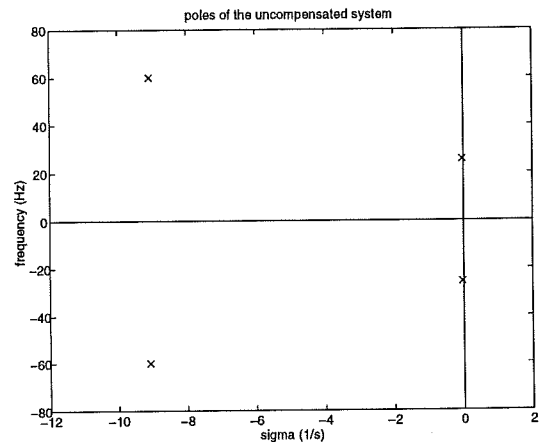


Figure 4.1: The electrical and mechanical poles for the uncompensated system.

These are shown in Figure 4.1. There is little coupling between the mechanical system and the electrical one. Because of this, two of the eigenvalues appear close to the eigenvalues of a separate mechanical system, that is, the poorly damped poles at 25.55 Hz, whereas the other two eigenvalues appear close to the poles of a separate electrical system, the 60 Hz poles. The eigenvalues are thus referred to as the mechanical ones and the electrical ones, respectively.

When a series capacitor is introduced, the electrical eigenvalues split into two subsynchronous ones, with a frequency less than 60 Hz, and two supersynchronous ones, with a frequency higher than 60 Hz. The frequencies of the eigenvalues depend on the degree of compensation.

Figure 4.2 shows how the subsynchronous and supersynchronous poles move when changing the degree of compensation, that is, the value of  $x_C$ . What happens to the mechanical eigenvalues is shown in

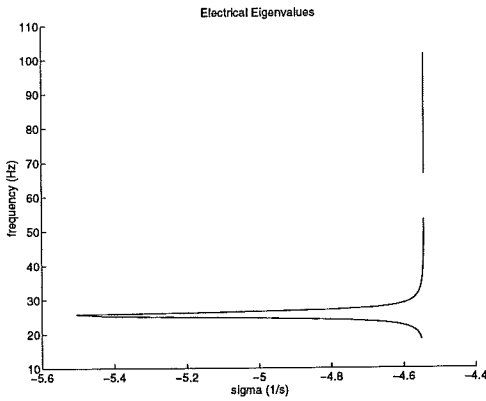


Figure 4.2: When a series capacitor is introduced, the electrical poles split into subsynchronous and super-synchronous ones.

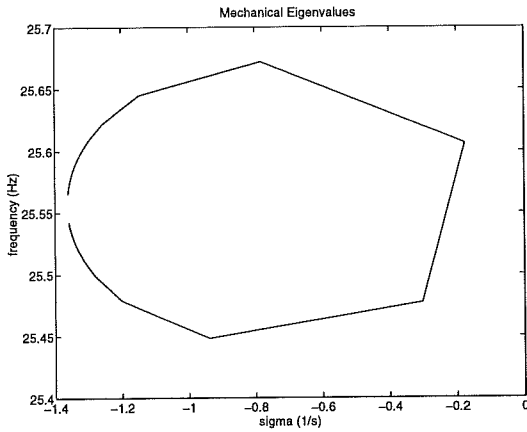


Figure 4.4: The system is stable if the damping factor  $d = 0.1$ .

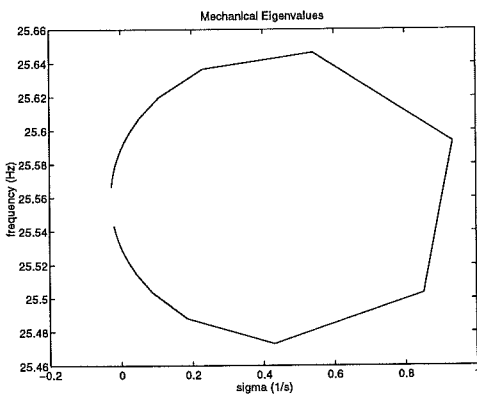


Figure 4.3: The mechanical eigenvalues make a loop into the right half plane as the frequency of the subsynchronous electrical poles get close to the one of the mechanical poles.

Figure 4.3. As the frequency of the subsynchronous eigenvalues get close to the mechanical frequency, the mechanical poles are forced into the right half plane, where they make a loop and return to the left half plane. The system is unstable for  $0.20 < x_C < 0.34$ .

It seems reasonable to believe that a higher damping of the mechanical system would move the loop further into the left half plane. That this is indeed the case can be seen in Figure 4.4, where the system is made stable by increasing the damping  $d$  from 0.002 to 0.1.

Introducing a virtual damping 50 times as large as the real damping is quite a drastical move. If it is

possible to make the loop smaller such a large  $d$  would not be necessary. The size of the loop depends on the electrical resistance. A higher resistance gives a smaller loop. It is of course not desirable to increase the resistance for the 60 Hz component, but with a simple feedback loop it is possible to create a virtual resistance for lower frequencies. The size of a loop for a system with a resistance five times as high ( $r_L = 0.1pu$ ) is shown in Figure 4.5.

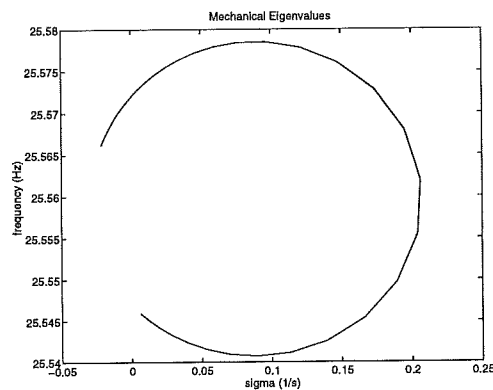


Figure 4.5: An  $r_L$  five times bigger makes the loop five times smaller.

By combining the two strategies a  $d = 0.02$  and an  $r_L = 0.1$  is sufficient to keep the loop completely in the left half plane, see Figure 4.6. These are much more realistic values for the parameters.

The linearized system explains qualitatively the behaviour of the system. The fact that the linearized system is unstable shows that it is not a non-linear

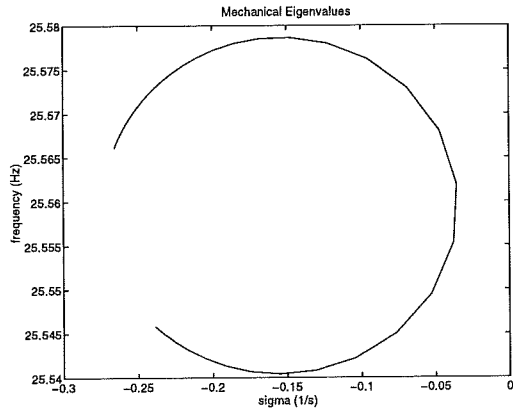


Figure 4.6: With  $r_L = 0.1$  and  $d = 0.02$ , the mechanical poles never reach the right half plane.

stability problem, but linear, which makes it less complicated.

## Chapter 5

# Control Strategies

The problem of torsional interaction can be dealt with in many ways. If the control means are located together with the generator, it is natural to measure the oscillations directly on the generator shaft and use that signal for the control. However, it is desirable to be able to control the system using only signals that are available locally at the location of the series capacitor. The control strategy should also be minimally dependent on the configuration of the transmission network.

### 5.1 Increased Damping

What makes it possible for the subsynchronous oscillations to grow is the poor damping of the mechanical system. The damping of the integrated system can thus become negative, something that is often referred to as *undamping*. The damping is determined by the parameters  $d$  (the mechanical part) and  $r_L$  (the electrical network). To increase either of these parameters would decrease the undamping of the system. A virtual damping is introduced if the electrical torque  $m_e$  has the same structure as the first term on the right hand side of Equation 2.6, also shown below. That is the term that holds the factor  $d$ .

$$\frac{2H}{\omega_N} \frac{d^2\theta}{dt^2} = -d \left( \frac{d\theta}{dt} - \frac{d\theta_t}{dt} \right) - k(\theta - \theta_t) + m_e + m_g$$

The rotor angle  $\theta$  was introduced in Chapter 2.

$$\theta = \theta_s + \Delta\theta$$

The rotor has the same synchronous speed as the turbine, but there is a phase lag  $\phi$  depending on the

magnitude of the load. If the load is constant, the phase lag is constant.

$$\begin{aligned} \theta &= \theta_t + \phi + \Delta\theta \\ \frac{d\theta}{dt} &= \frac{d\theta_t}{dt} + \frac{d}{dt}(\Delta\theta) \end{aligned}$$

The equation for the oscillations around the steady-state angle  $\theta_s = \theta_t + \phi$  reads:

$$\frac{2H}{\omega_N} \frac{d^2}{dt^2}(\Delta\theta) = -d \frac{d}{dt}(\Delta\theta) - k\Delta\theta + \Delta m_e + \Delta m_g$$

If it is possible to create an electrical torque, acting as a virtual damping with damping coefficient  $d_1$ ,

$$\Delta m_e = -d_1 \frac{d}{dt}(\Delta\theta) \quad (5.1)$$

the total damping will be  $d_{tot} = d + d_1$ .

The electrical torque depends on the line current  $i_L$  according to Equation 2.7:

$$\Delta m_e = \text{Im}(-\Delta i_L \Psi_s^*)$$

Now, a current that makes Equation 5.1 and Equation 2.7 equal may look like

$$\Delta i_L = j \frac{\Psi_s}{|\Psi_s|^2} d_1 \frac{d}{dt}(\Delta\theta) = j e^{j\theta} \frac{1}{\Psi} d_1 \frac{d}{dt}(\Delta\theta)$$

The system is controlled by the voltage source  $u_S$ . How should this be chosen in order to get the desired line current? Unless the oscillations are allowed to grow very large, the necessary current  $\Delta i_L$  is small. The stator and bus voltages can then be regarded as unaffected. In a linearized model they may then be short-circuited, see Figure 5.1. The control voltage  $u_S$  is given by:

$$u_S = r_L \Delta i_L + \frac{x_L}{\omega_N} \frac{d\Delta i_L}{dt} + \Delta u_C$$

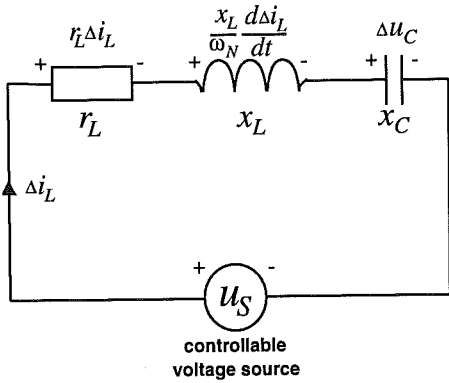


Figure 5.1: In a linearized model, stator and bus voltages are short-circuited.

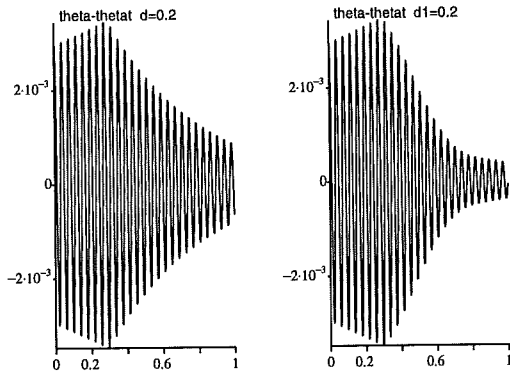


Figure 5.2: The control strategy used in the right picture adds a virtual damping torque that works as efficiently as a real damping torque.

$$\frac{d\Delta u_C}{dt} = \omega_N x_C \Delta i_L$$

The efficiency of this control strategy is shown in Figure 5.2. The left picture shows the uncontrolled system when the damping factor  $d = 0.2$ . To the right is shown the system with a  $d = 0.00256$ , controlled with the proposed strategy with a  $d_1 = 0.2$ . This gives an even better damping, which cannot be true. This is probably caused by the filterings in the estimation calculations, which may amplify the control signal marginally.

## 5.2 Controlling the Stored Energy

Another possible way to control the system is to look at the stored energy. If the energy of the system can be made to decrease in every moment, there can be no increasing oscillations. The energy can be divided in two parts, one containing the energy in the electrical network,  $W_{el}$ , and the other containing the energy of the rotor,  $W_m$ . This is a Lyapunov theory approach to the problem.

The expression for the electrical energy contains the energy in the inductor and the capacitor:

$$W_{el} = \frac{1}{2} x_L i_L i_L^* + \frac{1}{2} \frac{1}{x_C} u_C u_C^* \quad (5.2)$$

$$\frac{1}{\omega_N} \frac{dW_{el}}{dt} = \frac{1}{2} \frac{x_L}{\omega_N} \left( \frac{di_L}{dt} i_L^* + i_L \frac{di_L^*}{dt} \right) + \frac{1}{2} \frac{1}{x_C \omega_N} \left( \frac{du_C}{dt} u_C^* + u_C \frac{du_C^*}{dt} \right) \quad (5.3)$$

Taking the expression for  $\frac{d\Psi_s^*}{dt}$  in equation 2.4 and adding  $i_L \frac{d\Psi_s^*}{dt}$  to  $i_L^* \frac{d\Psi_s}{dt}$ , results in, using Equations 2.2, 5.2 and 5.3

$$\frac{1}{\omega_N} \left( i_L \frac{d\Psi_s^*}{dt} + i_L^* \frac{d\Psi_s}{dt} \right) = r_L (i_L i_L^* + i_L i_L^*) - (i_L^* u_S + i_L u_S^*) + \frac{1}{\omega_N} \left( i_L \frac{d\Psi_B}{dt} + i_L^* \frac{d\Psi_B}{dt} \right) + \frac{2}{\omega_N} \frac{dW_{el}}{dt} \quad (5.4)$$

The energy of the rotor part can be written

$$W_m = \frac{1}{2} \frac{2H}{\omega_N} \left( \frac{d\theta}{dt} \right)^2 + \frac{1}{2} k (\theta - \theta_t)^2 \quad (5.5)$$

$$\frac{dW_m}{dt} = \frac{2H}{\omega_N} \frac{d\theta}{dt} \frac{d^2\theta}{dt^2} + k \left( \frac{d\theta}{dt} - \frac{d\theta_t}{dt} \right) (\theta - \theta_t) \quad (5.6)$$

This, in combination with Equations 2.6 and 2.7, gives:



$$\begin{aligned} \frac{dW_m}{dt} + k \frac{d\theta_t}{dt} (\theta - \theta_t) &= -d \frac{d\theta}{dt} \left( \frac{d\theta}{dt} - \frac{d\theta_t}{dt} \right) \\ &+ \frac{1}{2j} \left( -\frac{d\theta}{dt} i_L \Psi^* + \frac{d\theta}{dt} i_L^* \Psi \right) \end{aligned} \quad (5.7)$$

The flux derivative is given by Equation 2.4:

$$\frac{d\Psi}{dt} = \hat{\Psi} e^{j\theta} j \frac{d\theta}{dt} = j \frac{d\theta}{dt} \Psi \quad (5.8)$$

Combining the last two equations results in

$$\begin{aligned} \frac{dW_m}{dt} + k \frac{d\theta_t}{dt} (\theta - \theta_t) &= -d \frac{d\theta}{dt} \left( \frac{d\theta}{dt} - \frac{d\theta_t}{dt} \right) \\ &- \frac{1}{2} \left( i_L \frac{d\Psi^*}{dt} + i_L^* \frac{d\Psi}{dt} \right) \end{aligned} \quad (5.9)$$

The total energy derivative is now given by adding Equations 5.3 and 5.9:

$$\begin{aligned} 2 \frac{dW}{dt} &= \\ &-2d \frac{d\theta}{dt} \left( \frac{d\theta}{dt} - \frac{d\theta_t}{dt} \right) - 2k \frac{d\theta_t}{dt} (\theta - \theta_t) \\ &-r_L (i_L i_L^* + i_L i_L^*) - (i_L^* u_S + i_L u_S^*) \\ &+ \frac{1}{\omega_N} \left( i_L \frac{d\Psi_B^*}{dt} + i_L^* \frac{d\Psi_B}{dt} \right) \end{aligned} \quad (5.10)$$

A control law that keeps the derivative negative would stabilize the system. To make the controllable part of Equation 5.10, that is  $-(i_L^* u_S + i_L u_S^*)$ , always negative, is the same as introducing a virtual resistance on the line. That does not, as mentioned before in Chapters 3 and 4, create an active damping of the mechanical system. A strategy that assures that the energy must decrease over each period is a less strict condition that might work better.

This method is not analysed any further. Neither is a common state feedback. A state feedback can affect only the two upper rows in the  $A$  matrix, Appendix B. Probably, a control structure similar to the one in Section 5.1 can be achieved with state feedback. An analysis of the resulting closed loop matrix,  $A - BL$ , can explain what happens with the poles when a virtual damping or a virtual impedance is introduced. This is definitely worth examining.

## Chapter 6

# Some Key Questions

The control strategy proposed in Section 5.1 requires knowledge about the rotor angle  $\theta$  and its derivative  $\frac{d\theta}{dt}$ , in order to steer in the right direction.

1. Is it possible to determine the position of the rotor without additional measurements, for instance, line-to-ground voltage?
2. If not so, what additional signal is to be measured and how should it be used?
3. Is it possible to achieve an actively damping torque without knowing the position of the rotor?

These questions will be discussed in the following three sections, respectively.

### 6.1 Question 1

When measuring only line current and capacitor voltage, it is not possible to observe the stator terminal voltage vector  $E_S$  or the bus voltage vector  $E_B$ , but only the difference  $E_S - E_B$ . This is rather natural since this is the voltage across the transmission line. The two cases shown in Figure 6.1, for instance, results in the same line voltage. Thus, the direction of the line voltage vector does not yield sufficient information about the rotor angle,  $\theta$ . This requires knowledge about  $E_S$ .

The shape of  $E_S$  is given in the model description in Chapter 2:

$$E_S^s = \frac{1}{\omega_N} j \frac{d\theta}{dt} \hat{\Psi} e^{j\theta} = j(n_0 + \Delta n) \hat{\Psi} e^{j(\theta_s + \Delta\theta)}$$

$E_S$  can be written as

$$E_S^s = E_0^s + \Delta E_S^s$$

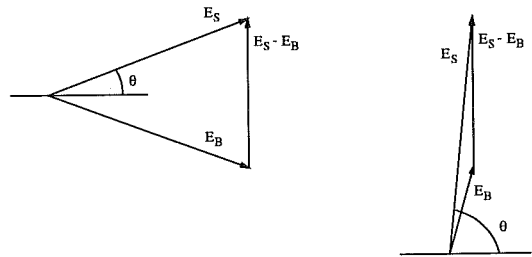


Figure 6.1:  $E_S$  is not uniquely given by measuring  $i_L$  and  $u_C$ . This gives only the line voltage  $E_S - E_B$ .

where  $E_0^s$  is a vector of constant length rotating at constant angular speed  $\omega_N$ .

$$E_0^s = \frac{1}{\omega_N} j \frac{d\theta_s}{dt} \hat{\Psi} e^{j\theta_s} = j n_0 \hat{\Psi} e^{j\theta_s}$$

$$\begin{aligned} \Delta E_S^s &= j(n_0 + \Delta n) \hat{\Psi} e^{j(\theta_s + \Delta\theta)} - j n_0 \hat{\Psi} e^{j\theta_s} \\ &\approx j e^{j\theta_s} \hat{\Psi} (j n_0 \Delta\theta + \Delta n) \end{aligned}$$

Now, suppose that

$$\Delta\theta = A \cos \omega t$$

$$\Delta n = \frac{1}{\omega_N} \frac{d\Delta\theta}{dt} = -\frac{\omega}{\omega_N} A \sin \omega t$$

$\Delta E_S^s$  performs an elliptic motion around  $E_0^s$ . The length of the main axes of the ellipse are in the ratio of  $\omega$  to  $\omega_N$ , with the shorter in the same direction as  $E_S^s$ . By locating the ellipse, the direction of  $E_S^s$  is given; see figure 6.2.

The problem is only that the truth is not that simple. The signal  $\Delta\theta$  is not completely cosine-shaped. Still, there may be some information to extract from

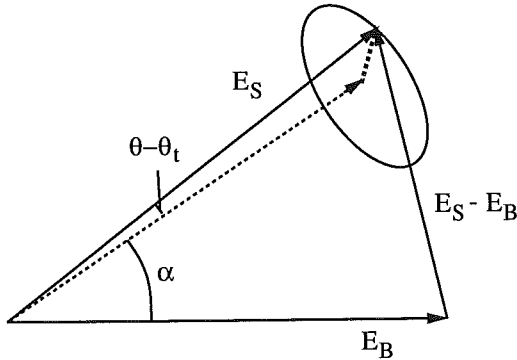


Figure 6.2: The result of the oscillations is that  $E_S$  performs an elliptic motion around the steady-state vector  $E_0$ . The main axes of the ellipse carries information about the direction of  $E_S$ .

it. However, a much more thorough examination is required.

If there is another way to get the position of the rotor, this would involve non-linear observer theory, which is far beyond this thesis.

## 6.2 Question 2

The problem with the case when only line current and capacitor voltage is measured is the absence of a fixed point to which voltages can be related. It seems natural to introduce a line-to-ground measurement signal to get around this.

This additional signal can be used in two ways.

1. A phase-locked loop (PLL) can be used to determine the synchronous rotor angle  $\theta_s$ . If the angle is known, the system can be transformed into rotor coordinates. Once in rotor coordinates a linear or non-linear observer can be used to determine  $\Delta\theta$  and  $\Delta n$ .
2. A non-linear observer can be used directly on the stator frame system. Such an observer avoids problems with the PLL, but meets other problems as shall be seen.

In Chapter 7 is described how different estimators may be designed.

## 6.3 Question 3

As shown when dealing with question 1, the line current (and the capacitor voltage) carry a great deal of information about the state of the system. It is not unlikely that there is a way to introduce an actively damping torque without knowing the rotor position. Recalling the electrical torque equation, Equation 2.7:

$$m_e = \text{Im}(-i_L \Psi_S^*)$$

As only the imaginary part creates a torque, the direction is not so crucial. In the control strategy proposed in Section 5.1, the real part is chosen to zero. This is not necessary, which makes it more probable that there are other ways to create an actively damping torque.

## 6.4 Conclusions

At this point, it is not known whether it is possible to create an actively damping torque without the discussed additional measurement signal. Thus, the rest of this report is based on the fact that line-to-ground measurement is available.

It seems a little awkward having to move back and forth on the line. First measure the potential at the capacitor, then derive the stator terminal voltage in order to get a control signal at the capacitor that affects the rotor in a certain way. There ought to be enough information in the line current to make it possible to control the system without estimating the rotor position. Such a method would of course be less sensitive to machine parameters and line impedance and would be more robust. Therefore, it would be an interesting task to tackle.

## Chapter 7

# Estimation Strategies

The two states that are not measurable are the rotor angle  $\theta$  and its derivative, or, rather, the shaft speed in pu,  $n = \frac{1}{\omega_N} \frac{d\theta}{dt}$ .

Recall the torque equation from Section 5.1:

$$\Delta m_e = Im(-\Delta i_L \Psi_s^*)$$

Only the imaginary part has any effect. This means that a small estimation error, like a phase lag, is not a problem as it only adds a real part to the factor  $\Delta i_L \Psi_s^*$ . The synchronous ‘steady-state’ rotor angle  $\theta_t$  is good enough an estimate for  $\theta$ .

If a line to ground voltage measurement is available, for instance to the right of the capacitor in Figure 2.1, it is possible to derive the stator terminal voltage  $E_S^s$ , using Kirchhoff’s Voltage Law

$$E_S^s = r_L i_L^s + \frac{x_L}{\omega_N} \frac{di_L^s}{dt} + u_C^s + u_m^s$$

where  $u_m^s$  is the line to ground voltage. The differentiation of the line current has to be carried out as a filtering. In the simulations this is arranged with a first order filter:

$$H(s) = \frac{s}{1 + sT}$$

$T$  is chosen so that  $H(s) \approx s$  for frequencies under consideration. All differentiations in this chapter are carried out in this way. The filtering gives a phase lag but, as mentioned before, if it is not too big it is not a problem. A discrete time estimator would allow other possibilities to solve the differentiation problem.

An analytical expression of  $E_S^s$  is given by Equation 2.4:

$$E_S^s = \frac{1}{\omega_N} \frac{d\Psi_s^s}{dt} = \frac{1}{\omega_N} j \frac{d\theta}{dt} \hat{\Psi} e^{j\theta}$$

The rotor angle  $\theta$  is now given as the argument of  $E_S^s$ . What is needed is actually only the factor  $e^{j\theta}$ . In the rest of this chapter, the shaft speed estimation will be discussed.

When estimating the shaft speed there are many possibilities. As mentioned in Chapter 6, there are essentially two ways to go—either transform the system into rotor coordinates, and then use an observer, or observe directly on the system in stator coordinates. Both strategies, and their advantages and drawbacks, will be discussed in this chapter, starting with the latter one.

## 7.1 Stator Frame Estimation

### 7.1.1 Rotor Angle Differentiation

The argument of  $E_S^s$  is  $\theta + \frac{\pi}{2}$ . This can be determined using a special arc tangent function, in many calculation programmes called ‘atan2’. This gives as a result an angle between  $-\pi$  and  $\pi$ . Differentiating this angle gives the shaft speed. There is a problem, because the angle is not continuous, but that can be solved easily.

### 7.1.2 Stator Voltage Integration

If  $E_S^s$  is integrated, the magnetic stator flux is achieved:

$$\begin{aligned} \int E_S^s dt &= \int \frac{1}{\omega_N} j \frac{d\theta}{dt} \hat{\Psi} e^{j\theta} dt = \\ &= \frac{1}{\omega_N} \hat{\Psi} e^{j\theta} + C = \frac{1}{\omega_N} \Psi_S^s + C \end{aligned}$$

where  $C$  is a complex integration constant, which can be removed with a high-pass filter. Multiplying  $E_S^s$  with the conjugate of the filtered flux gives:

$$\begin{aligned} E_S^s * \frac{1}{\omega_N} \Psi_S^{s*} &= \\ &= \frac{1}{\omega_N} j \frac{d\theta}{dt} \hat{\Psi} e^{j\theta} \frac{1}{\omega_N} \hat{\Psi} e^{-j\theta} = j \frac{d\theta}{dt} \frac{\hat{\Psi}^2}{\omega_N^2} \end{aligned}$$

### 7.1.3 Stator Voltage Differentiation

Normalizing  $E_S^s$  yields a unit vector  $\hat{E}^s$ . If this is differentiated and then multiplied with the conjugate of the unit vector itself, the result gives  $\frac{d\theta}{dt}$ .

$$\begin{aligned} \hat{E}^s &= \frac{E_S^s}{|E_S^s|} = j e^{j\theta} \\ \frac{d\hat{E}^s}{dt} &= -\frac{d\theta}{dt} e^{j\theta} \\ \frac{d\hat{E}^s}{dt} * \hat{E}^{s*} &= j \frac{d\theta}{dt} \end{aligned}$$

The problem is that what is actually wanted is not  $\frac{d\theta}{dt}$  but  $\frac{d\Delta\theta}{dt} = \frac{d\theta}{dt} - \frac{d\theta_i}{dt}$ , which is only a small modulation. Thus  $\frac{d\theta}{dt}$  has to be determined very accurately. Small numerical errors result in an offset. This means that the differentiations and filterings can be hard to realize. The integration method also requires knowledge about the machine parameter  $\hat{\Psi}$ .

Figure 7.1 shows a simulation of the differentiation method. The offset problem is obvious. There also is a phase lag, much due to the filterings. Otherwise, the result is not so bad.

## 7.2 Rotor Frame Estimation

When performing the estimation in the rotor frame system, the problem with the small modulation can be solved. Switching to rotor coordinates the stator terminal voltage reads

$$E_S^r = \frac{1}{\omega_N} j \frac{d\theta}{dt} \hat{\Psi} e^{j\Delta\theta}$$

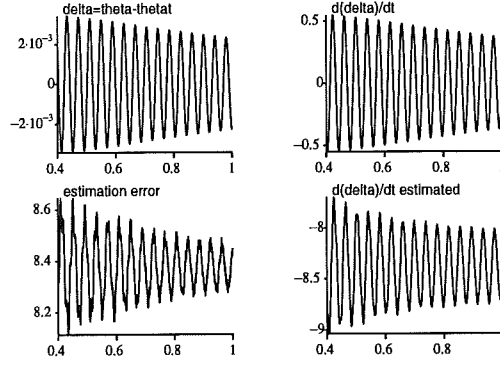


Figure 7.1: The method based on differentiation. The offset problem is clearly shown, while the rest of the estimation error is mainly due to the phase lag.

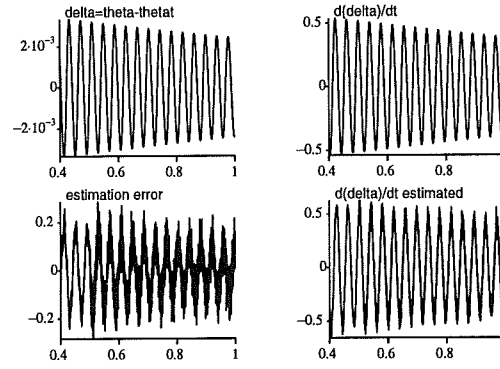


Figure 7.2: The angle estimated from the rotor frame stator terminal voltage has a small phase lag, but is good enough to use when controlling the system.

### 7.2.1 Stator Voltage Differentiation

The differentiation method gives

$$\begin{aligned} \hat{E}^r &= \frac{E_S^r}{|E_S^r|} = j e^{j\Delta\theta} \\ \frac{d\hat{E}^r}{dt} &= -\frac{d\Delta\theta}{dt} e^{j\Delta\theta} \\ \frac{d\hat{E}^r}{dt} * \hat{E}^{r*} &= j \frac{d\Delta\theta}{dt} \end{aligned}$$

The numerical problems with the small modulation are now avoided. This can be seen in Figure 7.2. The estimated angle is here used in the control law. The phase lag problem is still present but it is not so severe and the control law still works well.

## 7.2.2 Linear Estimation

If the problem of finding the rotor angle is solved, the best estimator is probably a common linear Kálmán filter [Åström90]. As the torsional oscillations do not have to be large to be damaging ( $< 0.1$  rad), a linearized model works well. The Kálmán filter theory is well-developed and a lot of mathematical tools can be used for the linear theory, for instance, MATLAB. A major drawback, however, is that the elements of the linearization matrix in Appendix B have to be known. That includes a number of machine parameters. The most crucial parameter is the resonance frequency of the mechanical system,  $\omega = \sqrt{\frac{k}{2H}}$ . Fortunately, this frequency can be determined very accurately.

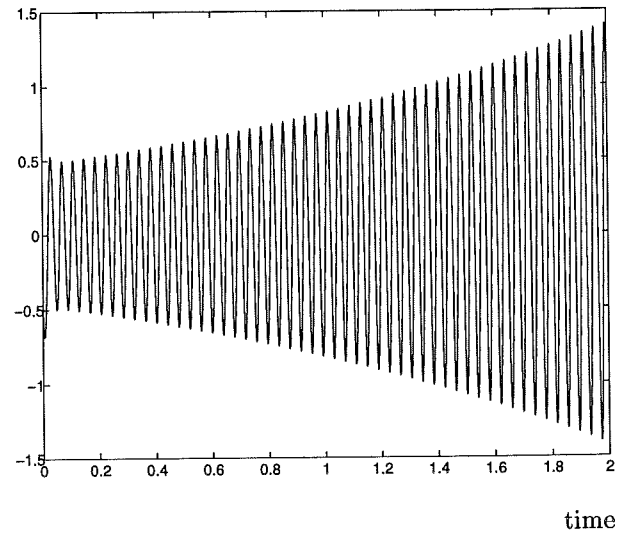
The MATLAB Control Toolbox was used to derive the Kálmán filter. Because of the problems with matrices when using SIMNON, the signals from the simulations in SIMNON were stored and transformed into a format readable by MATLAB. So the estimations were carried out by a discrete Kálmán filter in MATLAB. The estimated states were not used to control the system.

A problem with the Kálmán filter for a multiple output system is that there is not a unique solution. Therefore, the covariances of the states and outputs are used as weights. The most reliable states and outputs have most influence on the filter. For the filters used, all covariances were set equal, and all cross covariances were set to zero. Thus there was assumed to be no coupling between the states and signals, which probably is not quite true. Tests with different covariances exhibited approximately the same behaviour though.

Figure 7.3 shows the estimated shaft speed for the uncontrolled system. After a short start-up time, the estimation is really good. For the controlled system, the estimation is not quite as good, as shown in Figure 7.4. Problems with the sampling time when transforming the simulation data into MATLAB format showed that the filter is very sensitive to time delays in the control signal  $u_s^g$ . The result would be better if the simulation and the estimation were performed simultaneously in the same simulation programme.

The code for the Kálmán filter and the simulation is listed in Appendix C.

estimated shaft speed



estimation error

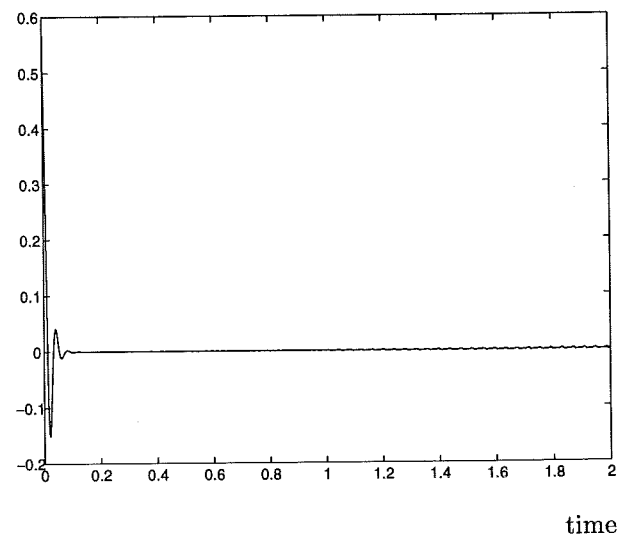
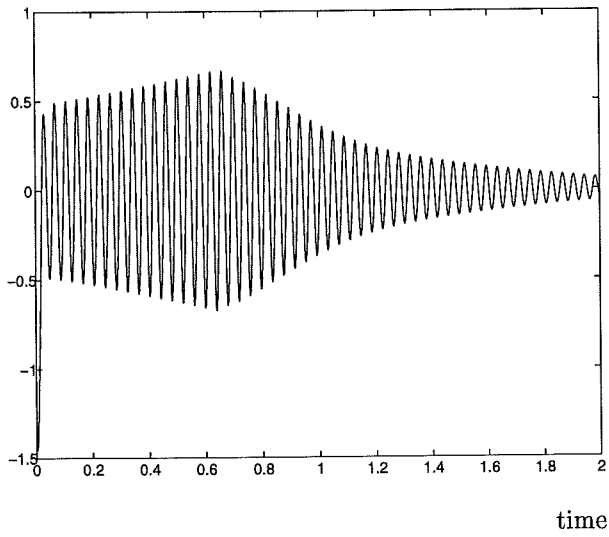


Figure 7.3: The Kálmán filter estimation and the estimation error for the shaft speed of the uncontrolled system.

estimated shaft speed



estimation error

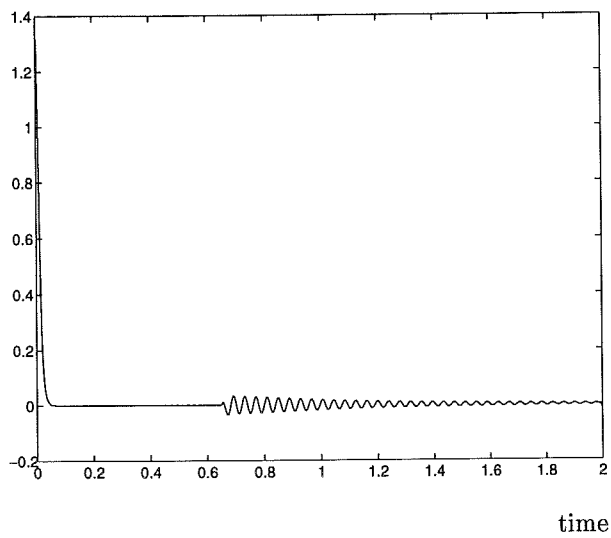


Figure 7.4: The Kálmán filter estimation and the estimation error for the shaft speed of the controlled system.

## Chapter 8

# Final Solution

All necessary parts of the controller, but the PLL, are described in this thesis. By combining them, it is possible to get a controller that works on the model from Chapter 2. A possible PLL design is described in [Ängquist3].

The model of the mechanical system is very much simplified. In reality, there are not only one turbine, but a lot of different turbines connected to each other. This gives rise to many different oscillation modes, whereas the model holds only one. The control strategy will probably not work satisfactorily for this reason. What can solve the problem is that the frequencies of the different modes are known very accurately. The system can be controlled by one controller for each oscillation mode using narrow banded filters.

The fact that the resonance frequencies of the mechanical system are well known also makes the Kálmán filter an excellent estimator. The filter requires, as mentioned in Section 7.2.2, accurate knowledge about the oscillation modes.

In the final solution proposed, see Figure 8.1, a PLL and a line to ground measurement is used to deter-

mine the steady-state rotor angle. When the angle is known, all signals are transformed into rotor coordinates. Now a Kálmán estimator gives the oscillative part of the rotor angle and shaft speed. A control signal can be determined and transformed back to stator coordinates. The control signal is also used as input for the Kálmán estimator.

There are a couple of things to work on with.

- Does the PLL design proposed in [Ängquist3] work satisfactorily? Does it give the synchronous rotor angle, unaffected by subsynchronous oscillations?
- How robust is the controller to parameter changes and noise?
- Does the control strategy work in a more sophisticated model with several oscillative modes?
- Does a common linear-state feedback give a more efficient and robust solution to the problem than the control strategy suggested in Section 5.1?

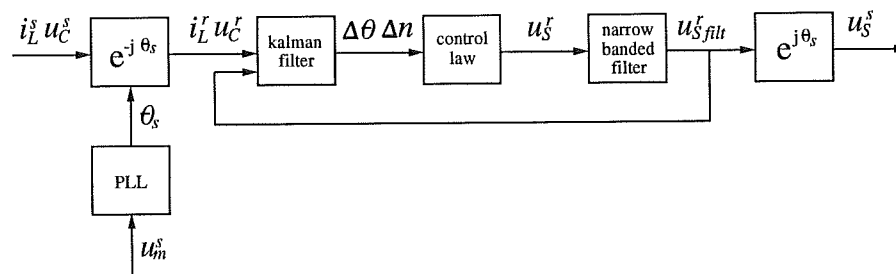


Figure 8.1: A diagram of a suggested controller structure



## Appendix A

# Analytical Tools

For the calculations and simulations, three analytical tools were used—SIMNON, MATLAB, and MAPLE.

**SIMNON** is a simulation program for both continuous-time and discrete-time simulations. The best thing about SIMNON is its simplicity. It is easy to implement the model and perform the simulations. One major drawback is that it does not handle matrices.

When storing signals for further treatment in MATLAB, the sampling time was not appropriate. This was avoided by including a discrete-time system, that did nothing. There were some problems with transforming the store file into a format, readable by MATLAB.

**MATLAB** is a calculation program superior in matrix calculations. It was used on the linearized model, for eigenvalue analyses, and for deriving and simulating the Kálmán filter. The control toolbox created by the Department of Automatic Control, Lund Institute of Technology, is a great help for control design.

**MAPLE** is a calculation program for symbolic algebra. It was used to linearize the model; see Appendix B. It is easy to use and a great complement to MATLAB, which handles only numbers.

## Appendix B

# Linearization Using MAPLE

The matrices from the linearization in Chapter 4 are derived using MAPLE. Section B shows the matrices and Section B shows how MAPLE was used to determine the  $A$  matrix.

### The Linearization Matrices

$$A = \begin{bmatrix} -\frac{\omega_{NRL}}{x_L} & \omega_N & -\frac{\omega_N}{x_L} & 0 & -\frac{\omega_N \hat{\Psi}}{x_L} n_0 \cos \Theta_0 & -\frac{\omega_N \hat{\Psi}}{x_L} \sin \Theta_0 \\ -\omega_N & -\frac{\omega_{NRL}}{x_L} & 0 & -\frac{\omega_N}{x_L} & -\frac{\omega_N \hat{\Psi}}{x_L} n_0 \sin \Theta_0 & \frac{\omega_N \hat{\Psi}}{x_L} \cos \Theta_0 \\ \omega_N x_C & 0 & 0 & \omega_N & 0 & 0 \\ 0 & \omega_N x_C & -\omega_N & 0 & 0 & 0 \\ 0 & 0 & 0 & 0 & 0 & \omega_N \\ \frac{\hat{\Psi}}{2H} \sin \Theta_0 & -\frac{\hat{\Psi}}{2H} \cos \Theta_0 & 0 & 0 & \frac{1}{2H} \left( -k + \hat{\Psi} ilre_0 \cos \Theta_0 + \hat{\Psi} ilim_0 \sin \Theta_0 \right) & -\frac{\omega_N d}{2H} \end{bmatrix}$$

$$B = \begin{bmatrix} \frac{\omega_N}{x_L} & 0 \\ 0 & \frac{\omega_N}{x_L} \\ 0 & 0 \\ 0 & 0 \\ 0 & 0 \\ 0 & 0 \end{bmatrix}$$

$$C = \begin{bmatrix} 1 & 0 & 0 & 0 & 0 & 0 \\ 0 & 1 & 0 & 0 & 0 & 0 \\ 0 & 0 & 1 & 0 & 0 & 0 \\ 0 & 0 & 0 & 1 & 0 & 0 \end{bmatrix}$$

$$X = (\Delta ilre, \Delta ilim, \Delta ucre, \Delta ucim, \Delta \theta, \Delta n)^T$$

$$U = (usre, usim)^T$$

## How MAPLE is Used

This section shows how MAPLE is used to linearize the system under consideration.

---

```

> fire:=(-psi*n*sin(theta)+psiB*sin(alpha)+usre-ucr-rl*ilre)*wN/xl+wN*ilim;

fire :=
      (- psi n sin(theta) + psiB sin(alpha) + usre - ucr - rl ilre) wN
      ----- + wN ilim
                        xl
-----
> flim:=(psi*n*cos(theta)-psiB*cos(alpha)+usim-ucim-rl*ilim)*wN/xl-wN*ilre;

flim :=
      (psi n cos(theta) - psiB cos(alpha) + usim - ucim - rl ilim) wN
      ----- - wN ilre
                        xl
-----
> f2re:=wN*ucim+wN*xc*ilre;

      f2re := wN ucim + wN xc ilre
      f2re := wN ucim + wN xc ilre
-----
> f2im:=-wN*ucr+wN*xc*ilim;

      f2im := - wN ucr + wN xc ilim
-----
> f3:=wN*n;

      f3 := wN n
-----
> f4:=1/2/H*(-wN*d*(n)-k*(theta)+ilre*psi*sin(theta)-ilim*psi*cos(theta));

      - wN d n - k theta + ilre psi sin(theta) - ilim psi cos(theta)
f4 := 1/2 -----
                        H
-----
> with(linalg);
Warning: new definition for norm
Warning: new definition for trace

```

[BlockDiagonal, GramSchmidt, JordanBlock, Wronskian, add, addcol, addrow, adj, adjoint, angle, augment, backsub, band, basis, bezout, blockmatrix, charmat, charpoly, col, coldim, colspace, colspan, companion, concat, cond, copyinto, crossprod, curl, definite, delcols, delrows, det, diag, diverge, dotprod, eigenvals, eigenvects, entermatrix, equal, exponential, extend, ffgausselim, fibonacci, frobenius, gausselim, gaussjord, genmatrix, grad, hadamard, hermite, hessian, hilbert, htranspose, ihermite, indexfunc,



```

> ucre:=0;          ilim := 0
> ucim:=0;          ucre := 0
> psiB:=psi;        ucim := 0
> psi:=1;           psiB := psi
> alpha:=0;         psi := 1
> usre:=0;          alpha := 0
> usim:=0;          usre := 0
> k:=946.12;        usim := 0
> d:=0.002056;     k := 946.12
> H:=6.92;          d := .002056
> x1:=0.83;         H := 6.92
> r1:=0.02;         x1 := .83
> wN:=evalf(2*Pi*60); r1 := .02
> theta:=0;         wN := 376.9911185
> n:=1;             theta := 0
>                   n := 1

```

---

```

> p:=charpoly(A,s);

```

```

p := .7744909444*1011 xc s16 - .1255145474*1016 xc + .6771940069*1011 s
+ .2754751312*1011 s2 + .3130158878*107 xc s3 - .3984006426*1011 xc s2
+ 310132.5562 s4 + .3066559262*107 s3 + 18.22425056 s5 + 342463.3818 xc s4
+ .2932029196*1011 xc s2 + .1642050198*1010 xc s2 + .7556306096*1015 xc
+ s6 + .5215190687*1015

```

---

```
> solve(p,s);
```

```
RootOf(3125000 _Z6 + 56950783 _Z5 + (1070198068125 xc + 969164238125) _Z4
+ (9781746493750 xc + 9582997693750) _Z3
+ (- 124500200812500000 xc + 86085978500000000 + 91625912375000000 xc2) _Z2
+ (5131406868750000 xc2 + 242028420125000000 xc + 211623127156250000) _Z
+ 236134565500000000000 xc2 - 3922329606250000000000 xc
+ 1629747089687500000000)
```

---

```
>
```

---

The last part is an attempt to find an analytical expression for the poles of the system. Unfortunately, the result is not of very much help.

## Appendix C

# Program Code

### SIMNON Code

The following SIMNON code was used for the simulations in Chapter 3.

---

```

CONTINUOUS SYSTEM rotor

INPUT me wN
OUTPUT theta thetai thetat thetati
STATE delta delta1                " delta=theta-thetat
DER ddelta ddelta1                " delta1=d(delta)/dt
TIME t

ddelta=delta1
ddelta1=wN/2/H*(-d*(delta1)-k*(delta)+me+mg)
thetat=wN/60*MOD(60*t,1)          " 0 < thetat < 2 pi

theta=thetat+delta
thetati=wN
thetait=wN+delta1

d:0.002056
k:946.12
H:6.92
mg:0

END

```

---

```

CONTINUOUS SYSTEM network

INPUT theta thetai wN thetat thetati usre usim
OUTPUT me Esre Esim ilrotre ilrotim ucrotre ucrotim
OUTPUT umrotre umrotim usrotre usrotim

STATE ilre ilim ucre ucim umre umim
DER dilre dilim ducre ducim dumre dumim

TIME t

```

```

Esre=-psihat*theta1*sin(theta)/wN          " Stator terminal voltage
Esim=psihat*theta1*cos(theta)/wN          "
EBre=-psiB*thetat1*sin(thetat-alpha)/wN  " Bus voltage
EBim=psiB*thetat1*cos(thetat-alpha)/wN    "
dilre=wN/XL*(Esre-RL*ilre-ucore+usre-EBre) "
dilim=wN/XL*(Esim-RL*ilim-ucim+usim-EBim)  "
ducre=wN*XC*ilre                           "
ducim=wN*XC*ilim                           "

me=psihat*(ilre*sin(theta)-ilim*cos(theta)) " Electrical torque

ilrotre=ilre*cos(thetat)+ilim*sin(thetat)  "
ilrotim=ilre*(-sin(thetat))+ilim*cos(thetat) " Transfers il and uc
ucrotre=ucore*cos(thetat)+ucim*sin(thetat)  " into rotor coordinates
ucrotim=ucore*(-sin(thetat))+ucim*cos(thetat) "

dumre=1/T1*(EBre-usre-umre)                " Additional line-ground voltage measur
dumim=1/T1*(EBim-usim-umim)                "      um = 1/(1+sT1)*(EB-us)

umrotre=umre*cos(thetat)+umim*sin(thetat)  "
umrotim=umre*(-sin(thetat))+umim*cos(thetat) " Transfers um and us
usrotre=usre*cos(thetat)+usim*sin(thetat)  " into rotor coordinates
usrotim=usre*(-sin(thetat))+usim*cos(thetat) "

XL:0.83
RL:0.02
XC:0.287
psihat:1
psiB:1
alpha:0.25
T1:0.0004

```

END

---

CONNECTING SYSTEM gen

TIME t

me[rotor2]=me[network]

```

theta[network]=theta[rotor2]
theta1[network]=theta1[rotor2]
thetat[network]=thetat[rotor2]
thetat1[network]=thetat1[rotor2]

```

```

w0:376.9911
wN[network]=w0
wN[rotor2]=w0

```

END

---

MACRO test

SYST rotor network gen

```

STORE delta me[rotor] ilre ilrotre
SPLIT 2 2
ERROR 0.00001

```

INIT delta:2.8844E-3



INIT delta1[rotor]:0.10344

INIT ilre[network]:-1.51663E-2

INIT ilim[network]:-2.06085E-2

INIT ucre[network]:-1.09235E-2

INIT ucim[network]:7.65907E-3

INIT umre[network]:0.147435

INIT umim[network]:0.977762

SIMU 0 0.6 0.0005

ASHOW delta

TEXT 'theta-thetat'

ASHOW me

TEXT 'Electrical Torque, me'

ASHOW ilre

TEXT 'Current IL, stator frame'

ASHOW ilrotre

TEXT 'Current IL, rotor frame'

END

The code for the controller in Section 5.1:

---

```

CONTINUOUS SYSTEM volt
INPUT wN delta1 theta
OUTPUT usre0 usim0
STATE Y3re Y3im Y4re Y4im ucdre ucdim
DER dY3re dY3im dY4re dY4im ducdre ducdim

TIME t

idre=d1*(-sin(theta))/psihat*delta1      "      1 ddelta      j*theta
idim=d1*cos(theta)/psihat*delta1        " id=d1*---*-----*j*e
                                          "      psi      dt

                                          " ducd
ucdre=wN*XC*idre                         " ---- = wN*XC*id
ucdim=wN*XC*idim                         " dt
dY3re=wf*(-Y3re+ucdre)                  "
ucdref=(ucdre-Y3re)                     " High pass filters
dY3im=wf*(-Y3im+ucdim)                   " ucd
ucdimf=(ucdim-Y3im)                      "

dY4re=1/T1*(-Y4re+XL/wN/T1*idre)        "
dY4im=1/T1*(-Y4im+XL/wN/T1*idim)        "      XL did
                                          " us=RL*id+ --*--- + ucd
usre0=-Y4re+(XL/wN/T1+RL)*idre+ucdref   "      wN dt
usim0=-Y4im+(XL/wN/T1+RL)*idim+ucdimf   "

RL:0.02
XL:0.83
XC:0.287
T1:0.0004
wf:10
d1:0.02
psihat:1

END

```

---

The code for the estimation based on differentiation in the stator frame, Section 7.1.3. The result is shown in Figure 7.1.

---

```

CONTINUOUS SYSTEM estim1
INPUT ire iim ure uim wN umre umim
OUTPUT thetai delta1e
STATE Y1re Y1im Y2re Y2im
DER dY1re dY1im dY2re dY2im

TIME t

dY1re=1/T1*(-Y1re+XL/wN/T1*ire)          "      XL      s
dY1im=1/T1*(-Y1im+XL/wN/T1*iim)         " Es=--- ---- iL + RL iL + uC + um
                                          "      wN 1+sT
Esre=-Y1re+(XL/wN/T1+RL)*ire+ure+umre   "
Esim=-Y1im+(XL/wN/T1+RL)*iim+uim+umim   "

Ehat=SQRT(Esre^2+Esim^2+1E-10)
Erenorm=Esre/Ehat
Eimnorm=Esim/Ehat

dY2re=1/T1*(-Y2re+Erenorm)              "

```

```

dY2im=1/T1*(-Y2im+Eimnorm)           " differentiates Enorm
dErenorm=1/T1*(Erenorm-Y2re)         "
dEimnorm=1/T1*(Eimnorm-Y2im)         "

thetale=(Erenorm*dEimnorm-Eimnorm*dErenorm) " thetale is the estimated derivative
deltale=thetale-wN                   " of theta
thetae=atan2(-Esre,Esim)             "

RL:0.02
XL:0.83
XC:0.287
T1:0.0004
wf:10
psihat:1

END

```

---

The code for the estimation based on differentiation in the rotor frame, Section 7.2.1. The result is shown in Figure 7.2.

---

```

CONTINUOUS SYSTEM estim2
INPUT ire iim ure uim wN umre umim thetat
OUTPUT thetae deltale
STATE Y1re Y1im Y2re Y2im
DER dY1re dY1im dY2re dY2im

TIME t

dY1re=1/T1*(-Y1re+XL/wN/T1*ire)       " XL s
dY1im=1/T1*(-Y1im+XL/wN/T1*iim)       " Es=-- ---- iL + RL iL + uC + um
                                        " wN 1+sT
Esre=-Y1re+(XL/wN/T1+RL)*ire+ure+umre "
Esim=-Y1im+(XL/wN/T1+RL)*iim+uim+umim "

Esrotre=Esre*cos(thetat)+Esim*sin(thetat) " transforms Es into rotor coordinates
Esrotim=Esre*(-sin(thetat))+Esim*cos(thetat) "

Ehat=SQRT(Esrotre^2+Esrotim^2+1E-10)
Erenorm=Esrotre/Ehat
Eimnorm=Esrotim/Ehat

dY2re=1/T1*(-Y2re+Erenorm)
dY2im=1/T1*(-Y2im+Eimnorm)
dErenorm=1/T1*(Erenorm-Y2re)
dEimnorm=1/T1*(Eimnorm-Y2im)

thetale=(Erenorm*dEimnorm-Eimnorm*dErenorm)
deltale=thetale
thetae=atan2(-Esre,Esim)

RL:0.02
XL:0.83
XC:0.287
T1:0.0004
wf:10
psihat:1

END

```

---



```
ucrc0=0;  
ucim0=0;  
theta0=0;  
n0=1;
```

---

## References

- [Elgerd] Elgerd, Olle I. *Electric Energy Systems Theory—An Introduction*. McGraw-Hill Book Company, 2nd edition, 1982.
- [Anderson] Anderson, P. M., Agrawal, B. L., and Van Ness, J. E. *Subsynchronous Resonance In Power Systems*. IEEE Press, 1989.
- [IEEE] IEEE Subsynchronous Resonance Task Force of the Dynamic System Performance Working Group Power System Engineering Committee. *First Benchmark Model for Computer Simulations of Subsynchronous Resonance*. IEEE Transactions on Power Apparatus and Systems, Vol. PAS-96, no. 5, 1977.
- [Ängquist1] Ängquist, Lennart. *Representation av trefasstorheter med hjälp av komplexa rumsvektorer*. Technical Report, TR YTK 84-009, 1984. Internal
- [Ängquist2] Ängquist, Lennart. *Torsional Interaction SSR Mitigation*. Technical Report, TR POW/RS 94-002, 1994. Internal
- [Ängquist3] Ängquist, Lennart. *PLL for TCSC*. Technical Report, TR POW/RS 94-004, 1994. Internal
- [Åström90] Åström, Karl Johan and Wittenmark, Björn. *Computer Controlled Systems*. Prentice-Hall International Editions, 2nd edition, 1990.
- [Åström68] Åström, Karl Johan. *Reglerteori*. Almqvist & Wiksell AB, 2nd edition, 1968.

